NUMERICAL STUDY OF A VORAXIAL SEPARATOR FOR TREATMENT OF OIL SPILLS FROM VESSELS

Nguyen Viet Đuc[1],.Tran Hong Ha[2]
[1]Lữ đoàn 649, Cục vận tải, Tổng cục hậu cần,
[2] Đại học Hàng Hải Việt Nam
vietduc2909@gmail.com, tranhongha@vimaru.edu,vn

Abstract: *The paper introduces a numerical modeling of Voraxial Separator using Ansys Fluent. The Voraxial can specifically be used to separate contaminants, such as oil and sand from large volumes of liquids and without any pressure drop, enabling itself to be utilized in many different applications, both offshore and onshore. The Voraxial which is now available in several different sizes to process volumes is capable of two-way separation. The separator consists of a pip e with an internal diameter of 100 mm, in which the internal swirl element is placed. The swirl element is equipped with vanes, which generate the swirling flow. Downstream of the swirl element, due to the centrifugal force the oil flows towards the center of the 1.7 m long pipe. At the end of this pipe, the oil is extracted by a concentrically placed pick-up tube. Simulation results showed that the separator with 9 vans a good understanding of flow patterns of the swirling turbulent flow of oil-water mixtures. The methodology employed uses two- phase flow models that incorporate a coalescence model for oil droplets. The aim is to understand the oil-water separation capability of devices using swirling oil-water flows as function of key parameters, such as geometry, oil properties and operating conditions.*

Key words: *Voraxial separator, oil-water mixture.*

Classification number: *2.1*

1. Introduction

Oil spills pollute the marine environment, seriously affecting ecosystems, especially, ecosystems of mangroves, seagrasses, sandy tidal areas, lagoons and coral reefs. Oil pollution reduces the resilience and flexibility of ecosystems. Oil content in the water increases, oil films reduce the oxygen exchange capacity between air and water, reducing oxygen in the water, causing the balance of oxygen in the ecosystem to be upset. In addition, spills of toxins damage the ecosystem, which can cause ecological degradation. The new technology which is the voraxial separator in this search, it can operate at various ocean depths allowing the operator to be more flexibility to treat various types of spills such as oil existing on the surface or released on the ocean floor. By conducting the separation in the ocean, the vessels can skim the spilled oil 10 times longer since the amount of collected clean water in the holding tanks is reduced by 90%. The collected oil is discharged into a holding tank while the clean water remains in the ocean. This new technology enables any fleet of vessels to process significantly larger volumes of skimmed oil/water mixture, to collect more oil, to capture a higher concentration of oil, to remain in a longer operation, and to skim at faster forward speeds. The Voraxial can also be secured onboard the vessel to achieve the same flow rate efficiency. Similar to other auxiliary equipment on vessels such as firefighting hoses, the small footprint of the Voraxial is easily installed on supply vessels or tugboats, without interfering with the main function of the vessel. Swirling flow has been used successfully for other applications, such as the separation of solids from either gas [1] or liquid [2]. Liquid-liquid separation is more challenging due to the smaller density difference between the phases, high volume fraction of oil, poor coalescence and the danger of emulsion formation. Early research on hydro cyclones for liquid-liquid separation was carried out by Colman [3]. Further work on this type of separators is an active field of research, see [4] for instance. Dirkzwager [5] designed an axial hydro cyclone for in-line liquid-liquid separation. In an axial hydro cyclone the separated phases flow co-currently towards their respective downstream outlets. Single-phase experiments were carried out for this separator by Dirkzwager. Subsequently, Murphy et al. [6] compared these

measurements with numeric al results from two different computational fluid dynamics (CFD) packages. It was found that the main features of the flow were qualitatively well represented in the numerical simulations. However, large quantitative differences were observed between the numerical results mutually and between numerical results and experimental data. The in-line separator was further developed and investigated numerically by Delfos et al. [7]. This involved the design of an oil extraction outlet and the development of a computationally inexpensive numerical tool for the design of separator prototypes.

2. Methodology

A typical voraxial separator is shown in Figure 1.1. It consists of a rotating pipe, in which there is a rotor attached vane. This pipe is driven by an electric motor. Fluid flow passing through a rotational section acquires tangential momentum and enters the pipe in the form of a swirling flow. The swirling flow can be generated using mechanical devices that impart swirling motion to the fluid passing through them. This includes rotating vanes (blades) or grids and rotating tubes. By mean of the tangential inlet, the motor drives a rotating pipe, and it transfers the rotational motion to the fluid, then forms a swirling flow.

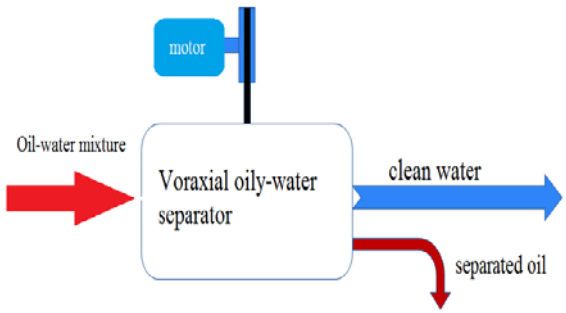

Figure 1. *System for separating oil from centrifugal water tube.*

2.1. Theory of vane design

For modeling vanes of the separator, the required velocity fields at the trailing edge should be calculated. The design process is to estimate the swirling flow of the mixture when it enters the rotating pipe. The azimuthal velocity distribution in the vane passage is shown in figure 2. An oil droplet will move quickly towards the center of the pipe. The drag force on the droplet is assumed to be given by Stokes'law [8]. In the present analysis, the axial and azimuthal components of the velocity difference are negligible compared to the radial component. The water phase is assumed to have the negligible radial velocity; therefore the velocity difference is equal to the radial velocity of the droplet. This drag force is balanced by the centrifugal body force acting on the droplet [8].

$$u_r = -\frac{\Delta\rho d^2 u_\theta^2}{18\mu r_d} \qquad (1)$$

Where: u_r: radial velocity; $\Delta\rho$: density difference; u_θ: azimuthal velocity; μ: viscosity; r_d: droplet radius.

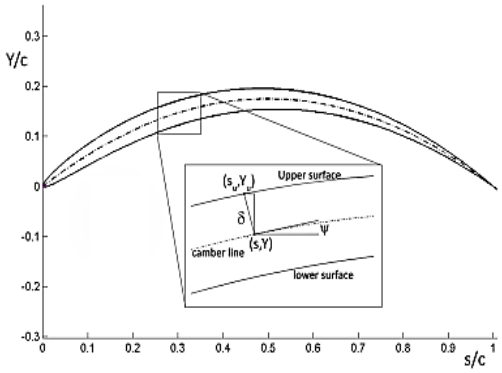

Figure 2 *Vans geography.*

The profile is in the form of a parabolic and has a maximum curvature of 50%. The profile is defined by the following function [8]:

$$Y(s) = \frac{4\Delta m}{c}(cs - s^2) \qquad (2)$$

Where: Y(s): Camber line shape; Δm: maximum distance from the chord line; s: coordinate along chord line; c: chord line of vanes.

The quantities are shown clearly in the figure. When s = 0, the thickness of the profile is calculated as follows [6]:

$$\delta(s) = \frac{\delta_{max}}{0.20}\left[a_0\sqrt{\frac{s}{c}} + a_1\frac{s}{c} + a_2\left(\frac{s}{c}\right)^2 + a_2\left(\frac{s}{c}\right)^3 + a_4\left(\frac{s}{c}\right)^4\right] \qquad (3)$$

Where: δ(s): the thickness distribution; δ_{max}: maximum thickness; a_0, a_1, a_2, a_3, a_4: coefficients.

When the maximum thickness is 4.8%, the coefficients are given in the following table:

Table 1. *Coefficients[8].*

a_0	a_1	a_2	a_3	a_4
0,2969	-0,126	-0,3516	0,2843	-0,1015

The top and bottom surfaces of the wing profile are now as follows [1]:

$$s_l(s) = s + \delta sin\psi(s)$$
$$Y_l(s) = Y(s) - \delta cos\psi(s) \quad (4)$$
$$s_u(s) = s - \delta sin\psi(s)$$
$$Y_u(s) = Y(s) + \delta cos\psi(s)$$

Where: $s_l(s)$, $s_u(s)$: lower and upper coordinates along the chord line; $Y_l(s)$, $Y_u(s)$: lower and upper camber line shapes; ψ: gradient of camber line shape; δ: vane thickness distribution;

The angle of the upper and lower camber lines is determined by the formula:

$$\psi = \arctan(\frac{dY}{ds}) = \arctan\left[\frac{4\Delta m}{c}(c-2s)\right] \quad (5)$$

The shape of the wing profile is shown in figure 2. The angle of the wing profile compared to the horizontal is -33.1 degrees as shown in the figure. The relationship between these two quantities is expressed as follows [8]:

$$Y_i^{'} = \sqrt{s_i^2 + Y_i^2}\sin\left[\arctan(\frac{Y_i}{s_i}) - \frac{33.1}{180}.\pi\right] \quad (6)$$
$$s_i^{'} = \sqrt{s_i^2 + Y_i^2}\cos\left[\arctan(\frac{Y_i}{s_i}) - \frac{33.1}{180}.\pi\right]$$

Where u or l is the upper or lower camber line of the impeller in Descartes. The angle between the center line and the horizontal axis is 5^0. The horizontal length of the vane profile is 83.5mm. The number of vanes used for the separator was chosen as 9. The length of average line is 31.4mm. By installing with multiple vanes, it is easy to change the direction of flow and avoid splashing when passing through the vanes. However, if the number of vanes increases, the frictional and pressure losses will be greater.

$$x_{in} = R_{in}\cos(\frac{Y_i^{'}}{R_{in}})$$
$$y_{in} = R_{in}\sin(\frac{Y_i^{'}}{R_{in}}) \quad (7)$$
$$z_{in} = s_i^{'}$$

Where: R_{in}: radius of central body; x_{in}, y_{in}, z_{in}: coordinates of vane contour on central body; Y'_i: rotated y-coordinate of lower or upper (i = [l, u]) surface of cascade vane; s'_i: rotated s-coordinate of lower or upper (i = [l, u]) surface of cascade vane.

2.2. Modeling and meshing

For the flow simulations, a computational mesh has to be created. This was accomplished employing ANSYS Fluent 14.0. The flow domain is divided into a not too large number of large hexahedral volumes, called blocks. These blocks are themselves divided into hexahedral elements. Care is taken to comply with the mesh quality requirement such as minimum and maximum angles of the hexahedral elements, variation in volume between adjacent elements and values of y+ at the walls, without using an unacceptably large number of hexahedral elements. The result of the long procedure to generate, iteratively, an adequate grid is given here, along with some meshing strategies that have been developed while generating the mesh. The mesh on the surface of the vane block is shown in figure 3. The fine mesh near the solid walls can be seen at the intersection of the vanes with the central body. This refinement is essential to capture the production of turbulent kinetic energy in the shear layer next to the walls. The large deflection of the flow by the vanes in combination with the periodicity of the geometry necessitated the introduction of a point where three, instead of four, blocks connect in order to increase the element angle to acceptable values. This point can be seen just downstream of the vanes. For the same purpose the block edges are slightly curved at various locations. At the nose and tail of the valve block, all mesh lines

converge, leading to a region with small elements. A mesh without hanging nodes between the blocking interfaces is created to avoid interpolation between non-matching mesh parts. Such interpolation would lead to small wiggles in pressure and velocity and to increased computational time. To obtain such a mesh without hanging nodes, the 9 blocking structures of the 9 vane passages need to be connected in the center of the pipe further downstream. This mesh has 1.6 million hexahedral elements and is used for other case studies of this research.

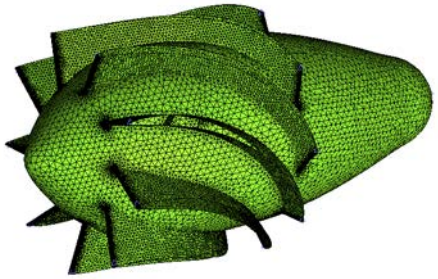

Figure 3. *Computational surface mesh.*

Table 1. *Input parameters.*

Specific gravity of water	840-960 kg/m^3
Oil in mixture	300-1000 ppm
Pipe diameter of separator (Voraxial pump and casing)	100 mm
Cross section area	3,14x0,05^2=0,00785 m^2
Axial velocity	2 m/s
Quality	56,52 m^3/h
Revolution	5500-6000 rpm

Figure 4. *Swirling flow rate.*

The figure shows the separating quality of the flow. The oil phase and water phase components receive an effective centrifugal force that will be separated from the mixture with the highest percentage of oil concentrated in the core of the flow. The density difference between the oil droplets and the continuous water phase causes the droplets to be pushed towards the center of the separator. The result of phase distribution is shown along the axis of the input data is v_z = 3m/s; 0.1% oil phase; the number of revolutions is 6000 rpm. Calculated process in 5000 loops with 250 time steps.

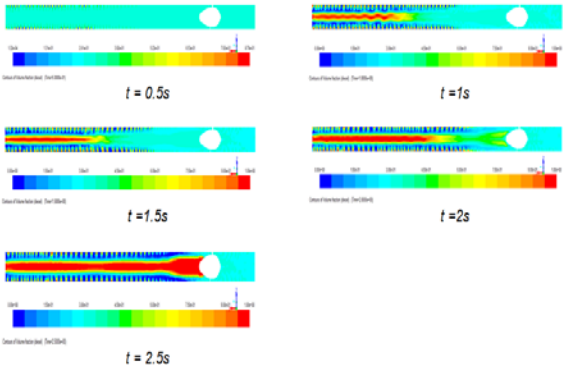

Figure 5. *Oil separation at 250 time steps.*

It can be seen that at the 250 time steps, the oil phase is concentrated in the center of the current and forms a middle layer of water and oil. This proves that the numerical approach to solve the problem is appropriate, but it must ensure the number of time steps needed.

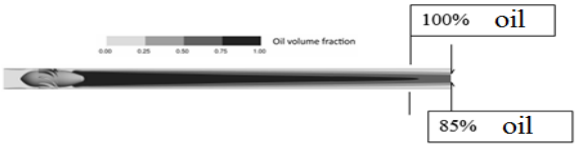

Figure 6. *Oil separation at 1000 time steps.*

The model for the co-current swirl separator is based on centrifugal buoyancy forces acting on the oil droplets, which are represented by the average droplet size. The inlet stream passes the swirl element and flows through the separator with a swirling flow pattern. The density difference between the oil droplets and the continuous water phase causes the droplets to be pushed towards the center of the separator (see figure 6). At the end of the separator, there is a light phase outlet where the inner fraction of the flow is extracted while the liquid outside of this radius passes the pick-up tube and exits through the heavy phase outlet.

Table 2. *Dimension of the collect oil pipe.*

Results gained after 1000 time steps with Δt = 0,001, error 10^{-4}	
d (smallest oil flow diameter-85% oil phase)	50 mm
L (suitable distance of oil collect pipe)	200 mm

3. Results and discussion

The results show that the set of data among the number of revolutions, the axial velocity and the flow is determined by structure of the separator. Therefore, changing one of these three parameters will result in the change of the remaining two parameters.

Table 3. *1000 ppm oil concentration.*

No	Revolution (rpm)	Velocity (m/s)	Capacity (m^3/h)	Oil specific gravity (kg/m^3)	d (mm)	Oil content in water outlet (ppm)
1	6000	2	56,52	840	26.7	10
2	6000	2	56,52	960	31.5	12
3	5500	1,5	42,39	840	36.8	13
4	5500	1,5	42,39	960	42.3	14

Table 4. *500 ppm oil concentration.*

No	Revolution (rpm)	Velocity (m/s)	Capacity (m^3/h)	Oil specific gravity (kg/m^3)	d (mm)	Oil content in water outlet (ppm)
1	6000	2	56,52	840	22	11
2	6000	2	56,52	960	27.3	13
3	5500	1,5	42,39	840	29.4	14
4	5500	1,5	42,39	960	33	15

Table 5. *300 ppm oil concentration.*

No	Revolution (rpm)	Velocity (m/s)	Capacity (m^3/h)	Oil specific gravity (kg/m^3)	d (mm)	Oil content in water outlet (ppm)
1	6000	2	56,52	840	15	9
2	6000	2	56,52	960	22	12
3	5500	1,5	42,39	840	24	13
4	5500	1,5	42,39	980	26	14

When the mixture changes oil concentration from 300 to 1000 ppm, the quality of separation still keep in good results that have oil content smaller than 15 ppm. The diameter of oil swirl flow is tendency larger when the oil concentration increase, so that collected oil pipe should change suitable diameter to collect oil out of the separator.

4. Conclusion

A separation system for oil-water separation has been studied in this paper. A design study has been carried out to develop an oil-water separator. In the study, a number of alternative configurations has been explored. Because of its in-line geometry and its relatively low pressure drop, the separator featuring an internal swirl element has been adopted for further research. The in-line aspect acilitates implementation in the existing pipe lines and allows for a compact design. For a pipe with an internal diameter of 100 mm, the distance between the after body of impeller and the entrance of the pick-up tube has been chosen as 1.7 m. This choice has been based on results of experiments. A method for designing future separator derived from the present design process. The current separator is a first design and improvement to its geometry can be made❑

Reference

[1]. A.J. Hoekstra. *Gas flow field and collection efficiency of cyclone separators*. PhD thesis, Delft University of Technology, 2000. ISBN 90-90143341-3.

[2]. D. Bradley. *The Hydrocyclone*. Pergamon Press, 1965.

[3]. D.A. Colman. *The Hydrocyclone for Separating Light Dispersions*. PhD thesis, University of Southampton, 1981.

[4]. C. Gomez, J. Caldentey, S. Wang, L. Gomez, R. Mohan, and O. Shoham. Oil/water Separation in Liquid/Liquid Hydrocyclones (LLHC): Part 1 - experimental investigation. *SPE Journal*, 7(4):353–372, 2002.

[5]. M. Dirkzwager. *A New Axial Cyclone Design for Fluid-Fluid Separation*. PhD thesis, Delft University of Technology, 1996.

[6]. S. Murphy, R. Delfos, M.J.B.M. Pourquie, Z. Olujic, P.J. Jansens, and F.T.M. Nieuwstadt. Prediction of strongly swirling flow within an axial hydrocyclone using two commercial CFD codes. Chemical engineering science, 62:1619–1635, 2007.

[7]. R. Delfos, S. Murphy, D. Stanbridge, Z. Olujic, and P.J. Jansens. A design tool for optimising axial liquid-liquid hydrocyclones. *Minerals Engineering*, 17(5):721–731, 2004.

[8]. Jesse Jonathan Slot, *development of centrifugal in line separator for oil-water flows, dissertation*, 2013.

[9]. Eyitayo Amos Afolabi, *experimental investigation and CFD simulation of multiphase flow in a three phase pipe separator*, 2012.

Ngày nhận bài: 2/3/2018
Ngày chuyển phản biện: 5/3/2018
Ngày hoàn thành sửa bài: 27/3/2018
Ngày chấp nhận đăng: 3/4/2018